Electron doping and phonon scattering in Ti1+xS2 thermoelectric compounds

Article

Accepted Version

It is advisable to refer to the publisher's version if you intend to cite from the work. See Guidance on citing.

www.reading.ac.uk/centaur

CentAUR

Central Archive at the University of Reading

Reading's research outputs online

Electron doping and phonon scattering in $Ti_{1+x}S_2$ thermoelectric compounds

M. Beaumale[1], T. Barbier[1], Y. Breard[1], G. Guelou,[2] A. V. Powell,[2] P. Vaqueiro[2], and E. Guilmeau[1*]

[1] *Laboratoire CRISMAT, UMR6508 CNRS ENSICAEN, 6 bd Marechal Juin-14050 CAEN Cedex 4 France.*

[2] *Department of Chemistry, University of Reading, Reading, RG6 6AD, United Kingdom*

* Corresponding author : emmanuel.guilmeau@ensicaen.fr ; Tel :+33 (0)2 31 45 13 67

Abstract :

Bulk polycrystalline samples in the series $Ti_{1+x}S_2$ (x = 0 to 0.05) were prepared using high temperature synthesis from the elements and spark plasma sintering. X-ray structure analysis shows that the lattice constant c expands as titanium intercalates between TiS_2 slabs. For x=0, a Seebeck coefficient close to -300 µV/K is observed for the first time in TiS_2 compounds. The decrease in electrical resistivity and Seebeck coefficient that occurs upon Ti intercalation (Ti off stoichiometry) supports the view that charge carrier transfer to the Ti 3d band takes place and the carrier concentration increases. At the same time, the thermal conductivity is reduced by phonon scattering due to structural disorder induced by Ti intercalation. Optimum ZT values of 0.14 and 0.48 at 300K and 700K, respectively, are obtained for x=0.025.

1. INTRODUCTION

The development of novel highly-efficient thermoelectric materials for solid-state energy conversion (refrigeration and electrical generation from waste heat) is currently at the core of worldwide research investigations [1]. The dimensionless thermoelectric figure of merit, ZT (ZT = $S^2T/\rho\kappa$, where S is the Seebeck coefficient, ρ is the electrical resistivity, κ is the total thermal conductivity and T the absolute temperature) is usually used to quantify the efficiency of a thermoelectric material. The total thermal conductivity (κ) is the sum of the lattice component (κ_l) and the electronic component (κ_{elec}). At present, the best performance for low and medium temperature ranges belong to Bi_2Te_3 intermetallics with optimum ZT values around 1 at 400K. However, the use of Bi_2Te_3 bulk thermoelectric materials for large scale applications needs to be reconsidered due to its toxicity, scarcity and high price. Thus, one of the current main interests is to develop new, non-toxic and cheap thermoelectric materials with comparable or higher efficiency for room and medium temperature ranges.

In the 2000's, Imai *et al.* have reported a large value of the Seebeck coefficient in TiS_2 (S = -250µV/K at 300K) combined with a relatively low and metallic-like resistivity (ρ=1.7 mΩ cm at 300K) [2]. In the following years, no great efforts have been devoted to this compound. Only recently, several studies have demonstrated the great potential of this compound below 400°C [3-5]. A power factor over 1.7 mW/mK^2 at room

3

temperature (RT) and ZT up to 0.5 at 800K have been reported for example. In addition, TiS_2 offers several advantages for practical applications such as low toxicity, low cost and low density (3.25 $g.cm^{-3}$).

TiS_2 belongs to the family of layered transition metal dichalcogenides (TMDC), TX_2, (where T is a transition metal atom from group IVb,Vb or VIb of the periodic table, X = S, Se, or Te) which have been fascinating compounds since the 1970s due to the rich variety of their physical properties [6-10]. It is built up by S-Ti-S layers which are stacked on top of each other and separated by a van der Waals' gap. Since the 1970s, the existence of stoichiometric TiS_2 is controversial although it is agreed that TiS_2 has either semimetal or semiconductor behavior [11-18]. In fact, it is well known that TiS_2 tends to grow metal rich and that the excess Ti atoms intercalate into the van der Waals' gap, leading to $Ti_{1+x}S_2$. Each excess Ti atom is assumed to be donor of four electrons to the conduction band. This off-stoichiometry is the main explanation of discrepancies in terms of physical and thermoelectric properties of the so-called TiS_2. Despite its rather simple composition, the synthesis of stoichiometric TiS_2 is complex. Atmosphere, pressure, temperature and synthesis conditions are among many factors which can affect sulfur volatilization. For example, Jeannin *et al.* firsly reported it was not possible to synthesize stoichiometric TiS_2 [19,20]. Later, Mikkelsen *et al.* [21] reported that the

ideal temperature for stabilizing stoichiometric TiS_2 is 632ºC. Above this temperature, the off-stoichiometry is inherent due to the high sulfur loss.

In the view point of thermoelectric properties, a wide range of Seebeck coefficient, electrical resistivity, and thermal conductivity values can be found for the so-called TiS_2 [2,3-5,11,22-28]. Thermoelectric properties are greatly dependent of the off-stoichiometry, more explicitly by the charge carrier concentration. As a result, a spread range of Seebeck coefficient values can be found in $1T$-TiS_2. For example, Thompson *et al.* reported the highest Seebeck coefficient for TiS_2 around -270µV/K whereas this coefficient is divided by around five (-60µV/K) in $Ti_{1.95}S_2$ [16].

It seems then of fundamental importance to understand the influence of Ti/S stoichiometry on the thermoelectric properties of TiS_2. If optimization of the power factor is possible by controlling the off-stoichiometry, *i.e.* the carrier concentration, it is also well know that the thermal conductivity needs to be reduced in these layered materials. By coupling the control of the Ti/S stoichiometry with the intercalation of Ti atoms in TiS_2 layers, optimized charge carrier concentration materials can be obtained while the thermal conductivity can be reduced in the same time. Based on this concept, we report here on the structural analysis and thermoelectric properties of materials in the $Ti_{1+x}S_2$ series.

2. EXPERIMENTAL SECTION

$Ti_{1+x}S_2$ dense ceramics were synthesized in a two step process. Mixtures of the pure elements (Alfa Aesar 99.5%) of stoichiometry $Ti_{1+x}S_2$ (x = 0, 0.005, 0.01, 0.015, 0.02, 0.025, 0.05) were heated in sealed fused silica tubes at 632 °C for 12h. The resulting powder is composed of plate-like grains of around 1-10 μm (in the *ab* plane). This powder was then ground and sieved down to 200 μm to remove large agglomerates.

The $Ti_{1+x}S_2$ powders were placed in tungsten carbide (WC) dies of 10 mm diameter and densified by Spark Plasma Sintering (SPS) (FCT HPD 25) at 600°C for 30 min under a pressure of 300 MPa. This temperature helps to prevent sulphur loss during densification while the high pressure of 300 MPa provides a high compaction, leading to final densities greater than 99% of the theoretical values. The final dimensions of the pellets are around 7 mm in thickness and 10 mm in diameter.

Structural characterization was carried out by X-Ray Diffraction (XRD) using a Panalytical Xpert Pro diffractometer (Cu Kα radiation) and the Rietveld refinements were performed using the FULLPROF program. The Seebeck coefficient (S) and electrical resistivity (ρ) were measured simultaneously in the temperature range of 300-700 K using a ULVAC-ZEM3 device under a partial Helium pressure. Hall effect experiments have been carried out using a Physical Properties Measurements Systems (PPMS, Quantum Design), in a magnetic field up to 7T. The heat capacity and thermal

diffusivity were analyzed using Netzsch STA 449-F3 and LFA-457 models, respectively. The thermal conductivity (κ) was calculated using the product of the density, the thermal diffusivity and the heat capacity. The lattice thermal conductivity was determined from the Wiedemann-Franz law (Lorenz number of $2.45.10^{-8}$ W.Ω.K^{-2}) by subtracting the electronic contribution to the total thermal conductivity ($\kappa_l = \kappa-\kappa_{elec}$).

The alignment of plate-like grains observed by Scanning Electron Microscopy (SEM ZEISS Supra 55) confirms that the crystalline *ab*- planes are slightly oriented perpendicular to the applied pressure direction [28]. Accordingly, *S*, ρ and κ were all performed along this direction (*i.e* in the plane perpendicular to the pressure direction).

3. RESULTS AND DISCUSSION

3.1. Structural analysis

The XRD patterns, recorded on powders of the obtained SPS pellets confirm that, for all *x* values in the range $0 \leq x \leq 0.05$, a single phase derived from TiS$_2$ is obtained (Fig. 1). All XRD patterns were well described in the trigonal space group $P\overline{3}m1$ of the TiS$_2$ host structure, as exemplified for the limit compound *x*=0.05 (Fig.2). The additional Ti atoms were distributed randomly over the octahedral positions in the van Der Waals' gap. Intercalation results in a systematic expansion of the unit-cell axis along the stacking direction and of the unit-cell volume. The *c* parameter increases from

7

5.678(1) Å for $x = 0$ to 5.715(1) Å for $x=0.05$. The increase is not linear as shown in

Fig. 3 with a plateau observed from $x = 0.015$ to $x = 0.025$. Such a behavior has been

previously observed and explained by the possible existence of a superlattice structure

over the c lattice [16, 29]. Special attention has been then paid on these compositions

and electron diffraction has been performed. Nevertheless no evidence of superstructure

has been detected in our compounds. This suggests indeed a step threshold evolution of

the cell parameters for low intercalation value.

3.2. Thermoelectric properties

The temperature dependences of the electrical resistivity and Seebeck coefficient in the

$Ti_{1+x}S_2$ series are displayed in Fig. 4. The electrical resistivity curves collected from 300

K up to 700 K demonstrate a general tendency towards more conducting behavior as the

Ti interstitial atom content increases. For instance, at 700 K, ρ decreases from 26.7

mΩ.cm to 0.72 mΩ.cm as x increases from $x = 0$ to $x = 0.05$. We note that the electrical

resistivity of the heavily doped compound $Ti_{1.05}S_2$ is almost independent of temperature.

The present results show some similarities to the behavior of Li_xTiS_2 [30], where a

charge-transfer mechanism was used to account for the observed phenomena. It is

reasonable to assume here that the valence electrons of the metallic titanium atoms

transfer to the Ti 3d band of the host after intercalation, leading to an increase of

8

electron concentration (Table 1) and enhancement of the metallic behavior of $Ti_{1+x}S_2$.

This suggestion is also consistent with the decreased Seebeck coefficient for the intercalated compounds.

We can also note that the magnitude of the electrical resistivity and the Seebeck coefficient is rather comparable between the three first member of the series (*i.e.* *x*=0, *x*=0.005 and *x*=0.01). The synthesis of samples has been repeated twice that confirmed this unexpected phenomenon.

Two main hypotheses can be drawn here.

First, this behavior has been previously explained by the existence of residual electrons associated to "displacement defects" [11,31]. For low x, Ti atoms move to the van der Waals' gap leaving behind Ti vacancies. These vacancies are supposed to be electron acceptors contrarily to Ti interstitials that are donors. For low *x* ($x \leq 0.01$), the number of acceptors (Ti vacancies) are not negligible compared with the donors (Ti interstitial) which explain the similar values obtained for *x*=0, *x*=0.005 and *x*=0.01. However, for *x* > 0.01, Ti interstitial process predominates which results in a low resistivity due to the larger content of electrons introduced in the conduction band. In other words, the residual carriers dominate at low x but make a negligible contribution to the total carrier concentration for x > 0.01.

A second hypothesis, which is the more likely explanation than the compensation

outlined above, concerns the titanium oxidation during SPS. This oxidation reaction induces the formation of a small content of TiO_{2-y} phase, as shown previously in Cu_xTiS_2 compounds [4]. If TiO_{2-y} traces have not been systematically detected in the XRD patterns of our samples (usually in the detection limit), the oxidation most probably originates from hydroxide or H_2O adsorption on the powder after sealed tube synthesis. As a consequence, the Ti content between the layers decreases due to the oxidation reaction during SPS and induces a decrease in carrier concentration, corresponding to an increase in Seebeck coefficient and electrical resistivity. Therefore, the slight increase in carrier concentration induced by off-stoichiometry is balanced by the titanium de-intercalation during SPS (decrease in carrier concentration). The first three members of the series have then quite similar properties. The saturation of $|S|$ close to 300 µV/K also indicates that the stoichiometric composition is certainly achieved (or very close).

These results are also confirmed by Hall effect measurements as presented in Table 1. The measured carrier concentration values are indeed very close for x=0, x=0.005 and x=0.01, as compared to the other members of the series whose values increase with Ti content.

Certainly, the first three members of the series possess the highest absolute value of Seebeck coefficient (S ~ 280-295 µV/K at 300K) of the $Ti_{1+x}S_2$ series. To the best of our

knowledge, such a magnitude of the Seebeck coefficient has not been reported before in bulk or single crystals of TiS_2. This new result is also supported by low c cell parameters ranging between 5.678 Å and 5.685 Å as compared to 5.695 Å reported for a Seebeck coefficient of -270 µV/K [16]. The low carrier concentration measured in our samples with a minimum value of 0.11×10^{21} cm^{-3} for $x=0$ confirms also the high value of Seebeck coeffcient. The lowest carrier concentration of 0.22×10^{21} and 0.28×10^{21} cm^{-3}, i.e. twice higher, were solely reported by Kukkonen *et al.* [11] and Imai *et al.*[2] in TiS_2 single crystals.

If we compare our data with previous studies, our results are closest to those reported by Thompson *et al.* in 1975 for single crystals. As we can observe from Fig. 5, a wide range of Seebeck coefficient values ranging from -38 µV/K for Li *et al.* [25] to -270 µV/K for Thompson *et al.* [16] have been reported for the so-called TiS_2, whilst intermediate values of *ca.* -160 µV/K and -80 µV/K were obtained by Guilmeau *et al.* [4] and Wan *et al.* [3] respectively. Of course, the main explanation of such a large variation in Seebeck coefficient values comes from differences in sample preparation that leads to different Ti/S ratios due to sulphur loss.

We also can note that for $x > 0.03$, reports by different authors are more in agreement with each other. For instance, the divergence in the magnitude of the Seebeck coefficient for $x = 0.03$ is only 40 µV/K (-40µV/K for Ohta *et al.* [5] to -80 µV/K for

Thompson *et al.*[16]) whereas this divergence is around 240 µV/K for a so-called TiS_2.

As a general trend, our values of Seebeck coefficient are in good agreement with literature data.

The temperature dependence of the power factor (PF) for $Ti_{1+x}S_2$ materials is presented in Fig. 6. For $0 < x < 0.025$, the power factor decreases with temperature. For $x = 0.025$ and $x = 0.05$, the PF is almost temperature independent due to a more metallic behaviour, as observed in the temperature dependence of the electrical resistivity. Optimum power factors of 1.66 mW/mK^2 at 300K and 1.04 mW/mK^2 at 700K are found for x=0.015 and x=0.02, respectively. The temperature dependence of the power factor for x=0.015 and x=0.02 is also rather similar to recent results for Cu_xTiS_2 compounds [4]. It confirms the significant impact of the off-stoichiometry and carrier concentration on the thermoelectric performances.

As for other intercalated TiS_2 compounds like Cu_xTiS_2 [4] and Nd_xTiS_2 [24], the presence of titanium in the intercalation sites decreases the lattice part of the thermal conductivity. Although the electronic contribution of the thermal conductivity increases with x due to charge carrier doping, the Ti intercalation between the TiS_2 layers generates disorder and phonon scattering even for a small excess of titanium. As shown

in Fig 7a. and 7b., the lattice and total thermal conductivity respectively decrease with

Ti off-stoichiometry. As reported recently by Wan *et al.* [3] in $(MS)_{1+x}(TiS_2)_2$ (M=Pb,

Bi, Sn) misfit layer compounds, the decrease in the lattice thermal conductivity may be

linked to the weak interlayer bonding and disruption of periodicity of the TiS_2 layers in

the direction perpendicular to the layers by the intercalated Ti layers. The magnitude of

the κ_l reduction (74% in the present study from $x = 0$ to $x = 0.05$ at 300 K) through Ti

intercalation is in good agreement and even higher than reported data in intercalated

Cu_xTiS_2, Nd_xTiS_2 and misfit $(SnS)_{1.2}(TiS_2)_2$ compounds which exhibit a substantial

decrease of between 30% and 50% [4,24,3].

This result suggests that the creation of an intermediate layer even composed of

few intercalated metal cations is a highly efficient means to decrease the thermal

conductivity of TiS_2. We can note that the thermal conductivity of the heavily doped

compound $Ti_{1.05}S_2$ is almost independent of temperature with a constant κ value of 3

W/mK for over the whole temperature range, which confirms phonon scattering due to

additional structural disorder. Moreover, the presence of Ti or/and S vacancies inside the

S-Ti-S layers may also create additional defects.

Fig. 8 exhibits the temperature dependence of the dimensionless figure of merit *ZT* of

the $Ti_{1+x}S_2$ series. For all the specimens, the *ZT* value increases with increasing

temperature. For x=0.0 and x=0.05, the ZT values are in the same range, close to 0.1 at

700K. For intermediate compositions, the ZT value is enhanced reaching an optimum value of 0.48 at 700 K for $x = 0.025$. According to recent reports, it appears that the optimum ZT in TiS_2 and intercalated TiS_2 compounds is obtained for carrier concentrations ranging between 0.6×10^{21} and 4×10^{21} cm^{-3} [4,5]. Within this range, the temperature dependence of ZT is usually more pronounced at higher carrier concentration. To our knowledge, the present ZT value of 0.48 at 700 K is the highest achieved in TiS_2 systems. The strategy to combine structural disordering and tuning of carrier concentration outlined in this study is then promising for the preparation of TiS_2-based thermoelectrics with enhanced ZT values.

4. CONCLUSIONS

In the present study, we have shown that the partial intercalation of Ti atoms in the van der Waals' gap of TiS_2 which greatly enhances the thermoelectric properties. Using an optimized preparation of powders and densification by Spark Plasma Sintering at low temperature (600°C/300MPa), a wide range of non-stoichiometric compounds were prepared with prevention of sulfur deficiency. We report for the first time a Seebeck coefficient close to -300 µV/K, at a carrier concentration of 0.11×10^{21} cm^{-3}, that is

unprecedentedly low for TiS$_2$ compounds. Controlled Ti/S stoichiometry allowed optimization of the electrical properties with optimum power factors of 1.66 mW/mK^2 at 300 K and 1.04 mW/mK^2 at 700 K achieved for x = 0.015 and x = 0.02, respectively.The thermal conductivity is also drastically reduced by effective phonon scattering through Ti intercalation in off-stoichiometric compounds. The resulting ZT is enhanced up to 0.48 at 700 K for x=0.025.

References

[1] Snyder GJ, Toberer ES. Nature Mater 2008;7:105.

[2] Imai H, Shimakawa Y, Kubo Y. Phys Rev B 2001;64:241104.

[3] Wan C,Wang Y, Wang N, Koumoto K. Materials 2010;3:2606.

[4] Guilmeau E, Bréard Y, Maignan A. Appl Phys Let 2011;99:052107.

[5] Ohta M, Satoh S, Kuzuya T, Hirai S, Kunii M, Yamamoto A. Acta Materiala 2012;60:7232

[6] Mattheiss LF. Phys Rev B 1973;8:3719.

[7] Wilson JA, Yoffe AD. Advances in Physics 1969;18:193.

[8] Bromley RA, Murray RB, Yoffe AD. J Phys C 1972;5:759.

[9] Hébert S, Kobayashi W, Muguerra H, Bréard Y, Nunna R, Gascoin F, Guilmeau E, Maignan A. Phys Status Solidi A 2013;210:69.

[10] Koumoto K, Funahashi R, Guilmeau E, Miyazaki Y, Weidenkaff A, Wang YF, Wan CL. J Amer Ceram Soc 2013;96:1

[11] Kukkonen CA, Kaiser WJ, Logothetis EM. Chem Rev B 1981;24:1691.

[12] Klipsten PC, Bagnall AG, Liang WY. J Phys C Solid State Phys 1981;14:4067.

[13] Fang CM, de Groot RA, Haas C. Phys Rev B 1997;56:4455.

[14] Logothetis EM, Kaiser WJ, Kukkonen CA. Physica B 1980;80:193.

[15] Whittingham MS, Panella JA. Mat Res Bull 1981;16:37.

[16] Thompson AH, Gamble FR, Symon CR. Mat Res Bull 1975;10:915.

[17] Kobayashi H, Sakashita K, Sato M, Nozue T, Suzuki T, Kamimura T. Physica B 1997;237:169.

[18] McKelvy MJ, Glaunsinger WS. J Solid State Chem 1987;66:181.

[19] Jeannin Y, Benard J. Compt Rend 1959;248:2875.

[20] Jeannin Y. Compt Rend 1960;251:246.

[21] Mikkelsen JC, Nuevo Cimento, 1977;38:378.

[22] Amara A, Frongillo Y, Aubin MJ, Jandl S, Lopez-Castillo JM, Jay-Gerin JP. Phys Rev B 1987;36:6415.

[23] Gascoin F, Nunna R, Guilmeau E, Bréard Y. J All Comp 2012;521:121.

[24] Li D, Qin XY, Zhang J, Li HJ. Phys Lett A 2006;348:379.

[25] Li D, Qin XY, Liu J, Yang HS. Phys Lett A 2004;328:493.

[26] Abbott EE, Kolis JW, Lowhorn ND, Sams W, Rao A, Tritt TM. Appl Phys Lett 2006;88:262106.

[27] Beaumale M, Barbier T, Bréard Y, Raveau B, Kinemuchi Y, Funahashi R, Guilmeau E. J Elec Mater DOI: 10.1007/s11664-013-2802-x, . p.1-7.

[28] Beaumale M, Barbier T, Bréard Y, Hébert S, Kinemuchi Y, Guilmeau E. J Appl Phys 2014;115:043704.

[29] Chianelli RR, Dines MB, Inorg Chem 1978;17:2758.

[30] Julien C, Samaras I, Gorochov O. Phys Rev B 1992;45:13390.

[31] Takeuchi S, Katsuta H. J Jap Inst Metals 1970;34:758.

Table Caption

Table 1. c unit-cell parameter, carrier concentration n at 300K, electrical resistivity (ρ), Seebeck coefficient (S), thermal conductivity (κ), lattice thermal conductivity (κ_l), power factor (PF), and figure of merit ZT at 700K in $Ti_{1+x}S_2n$ series.

Figure Caption

FIG. 1. XRD patterns in the series $Ti_{1+x}S_2$.

FIG. 2. Rietveld refinement of powder X-ray diffraction profile of $1T$-$Ti_{1.01}S_2$. R_{Bragg}=2.33, χ^2=2.29.

FIG. 3. Variation of c lattice parameters and unit-cell volume versus x in the $Ti_{1+x}S_2$ series.

FIG. 4. Temperature dependence of the electrical resistivity and Seebeck coefficient in the series $Ti_{1+x}S_2$.

FIG. 5. Seebeck coefficient as a function of x in $Ti_{1+x}S_2$ at 300 K of our study, along with those previsously reported.

FIG. 6. Temperature dependence of the power factor in the series $Ti_{1+x}S_2$.

FIG. 7. Temperature dependence of the lattice thermal conductivity (κ_l,) and total thermal conductivity (κ),in the series $Ti_{1+x}S_2$

FIG. 8. Temperature dependence of the figure of merit ZT in the series $Ti_{1+x}S_2$.
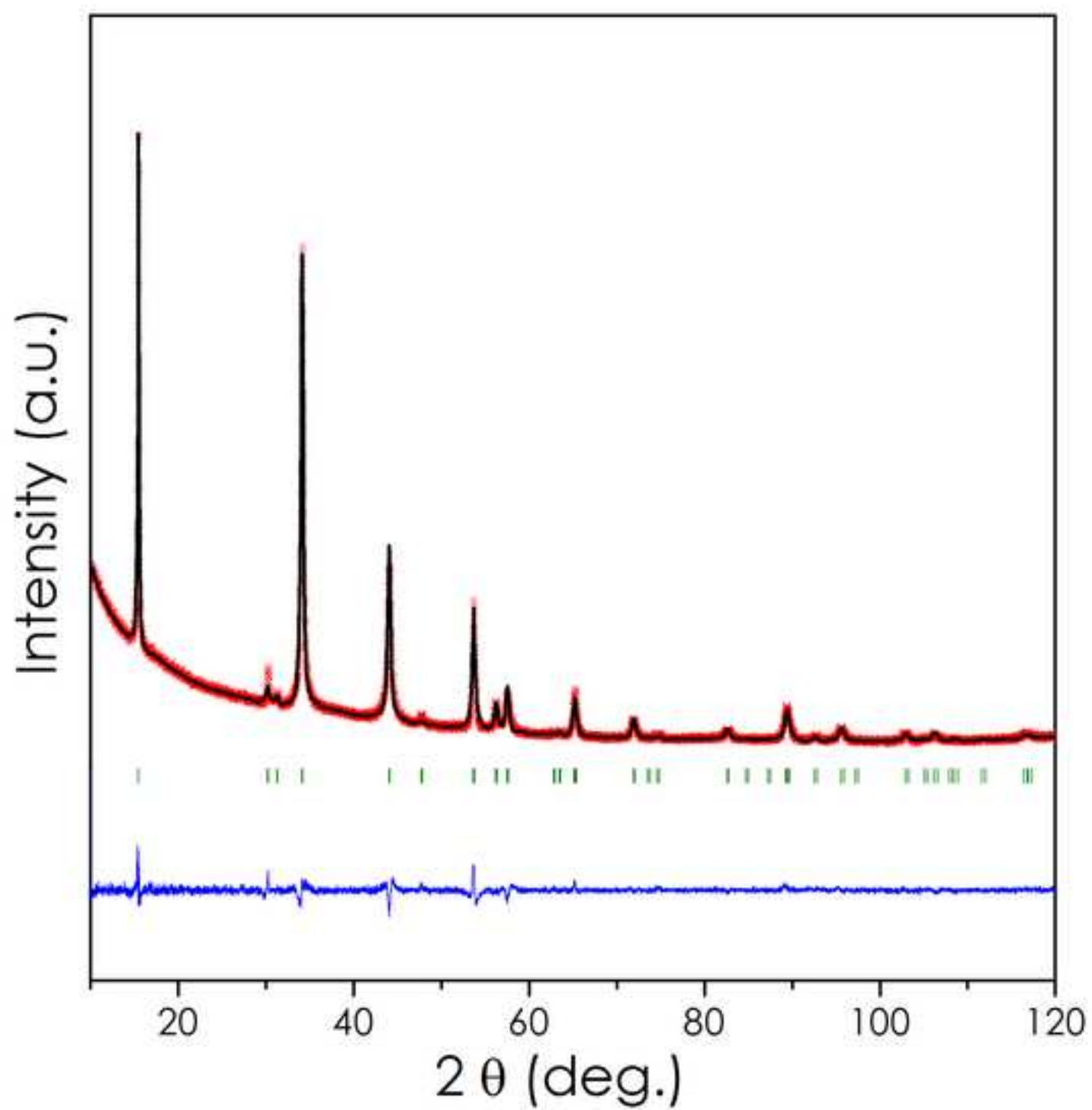
Figure1
Click here to download high resolution image
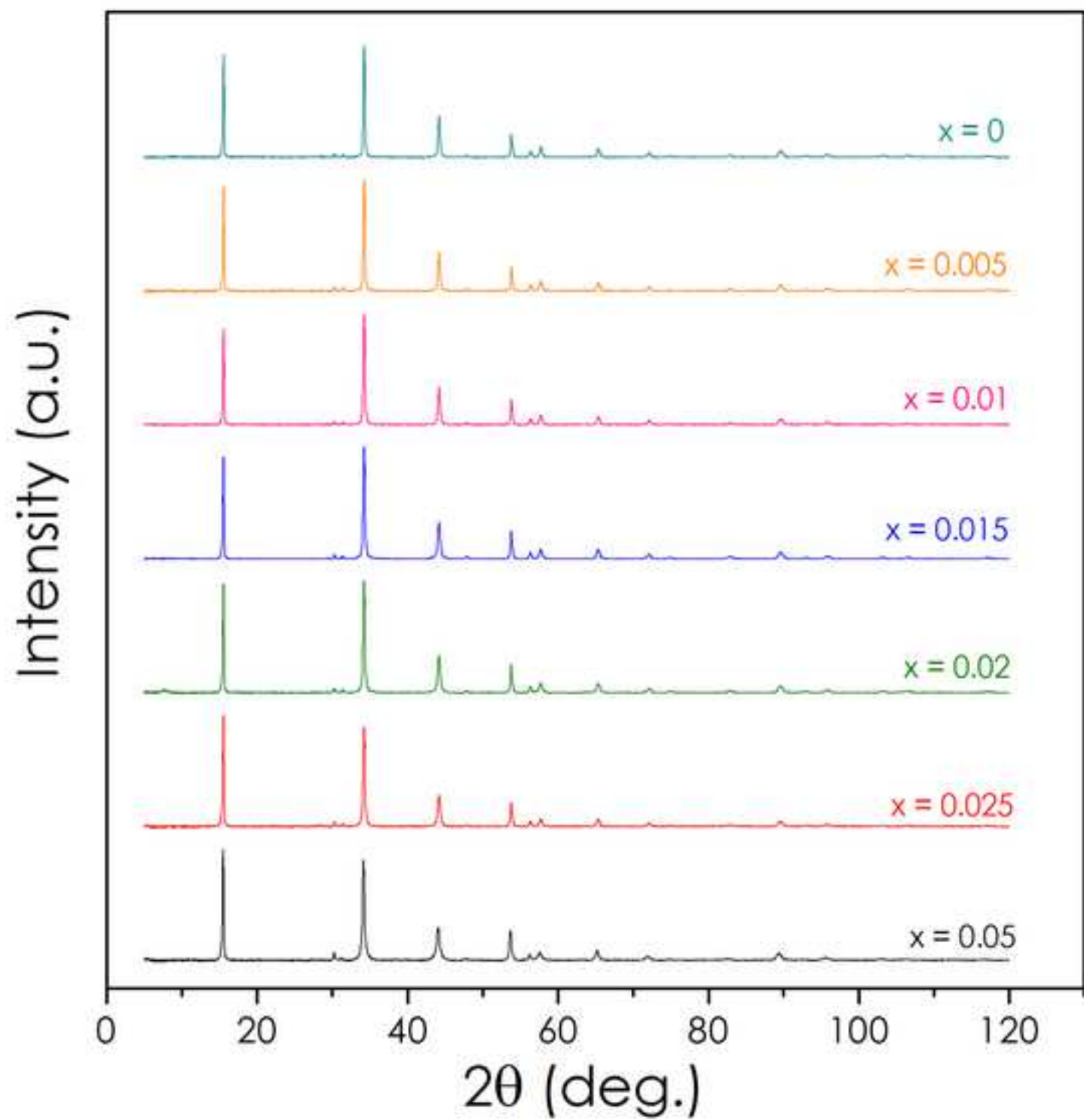
Figure3
Click here to download high resolution image

Figure4
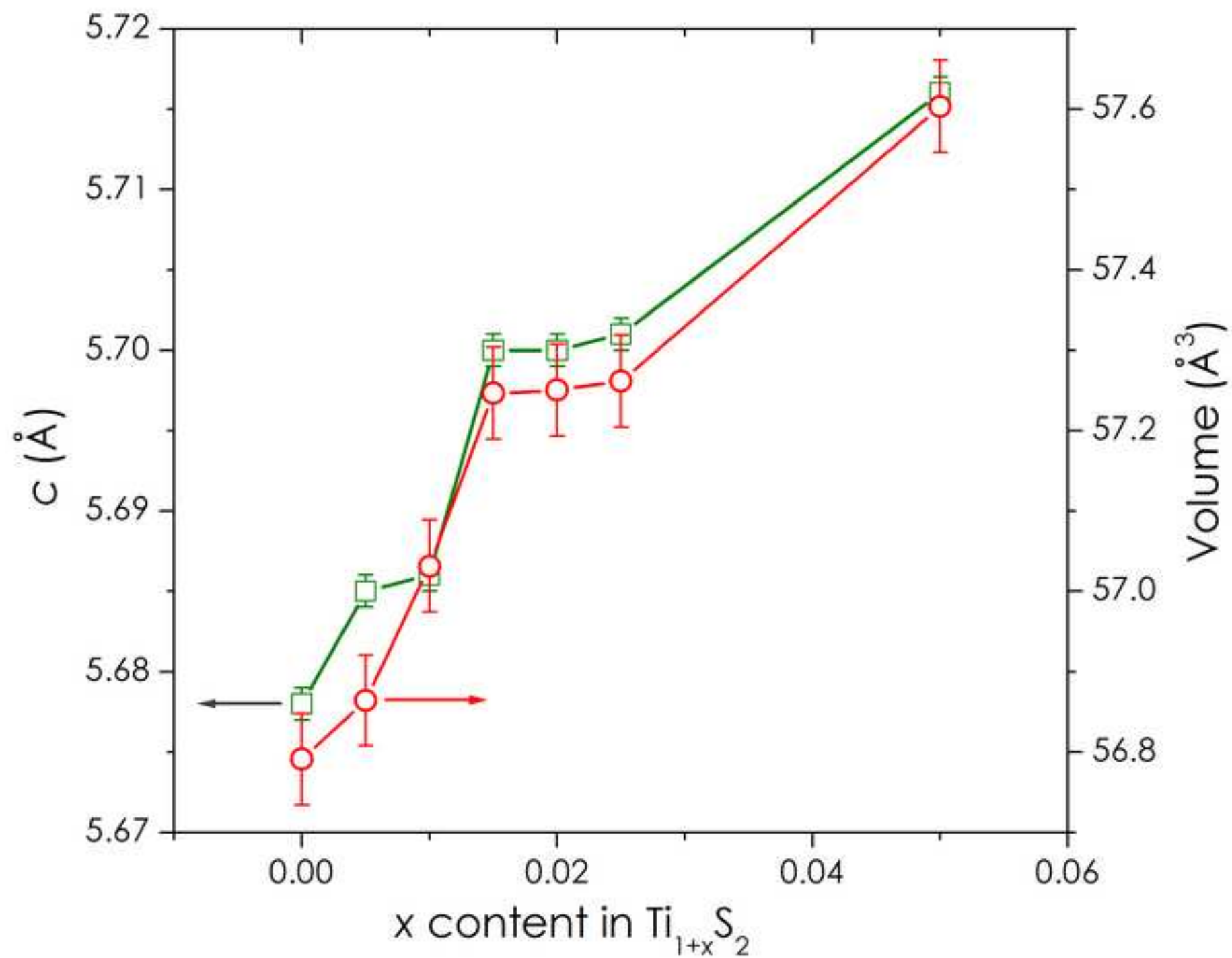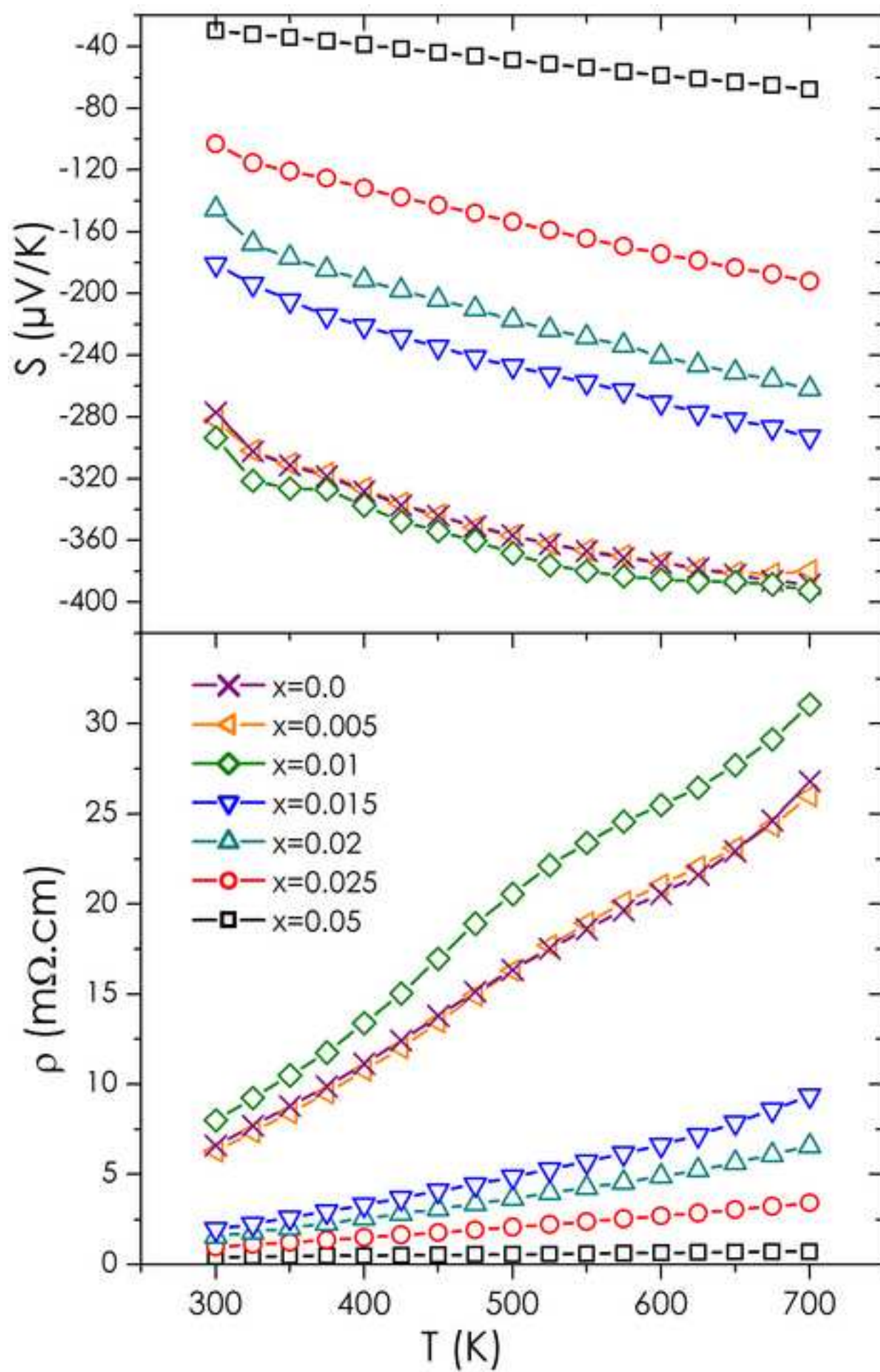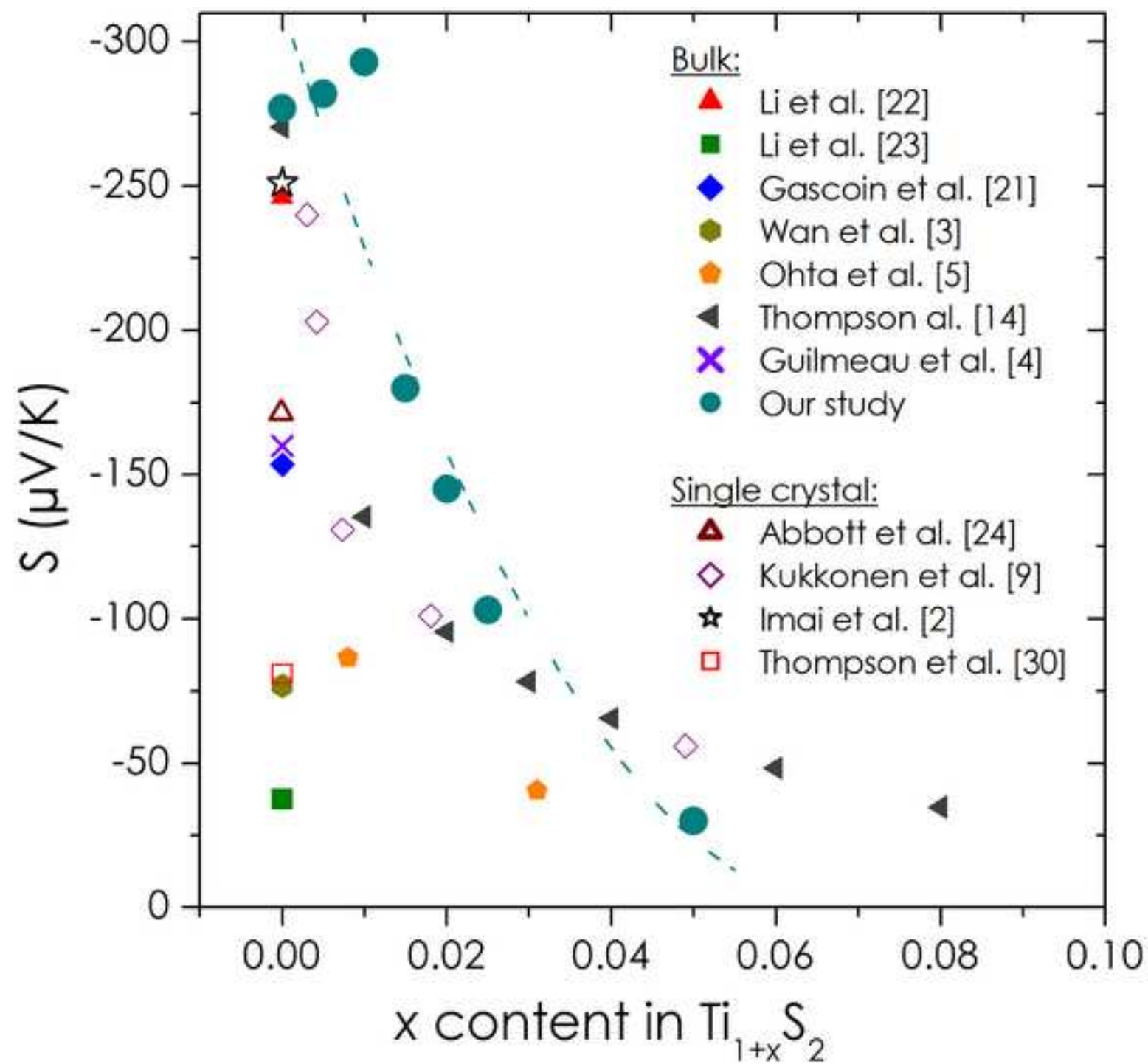**Click here to download high resolution image**

Figure5
Click here to download high resolution image

Figure6
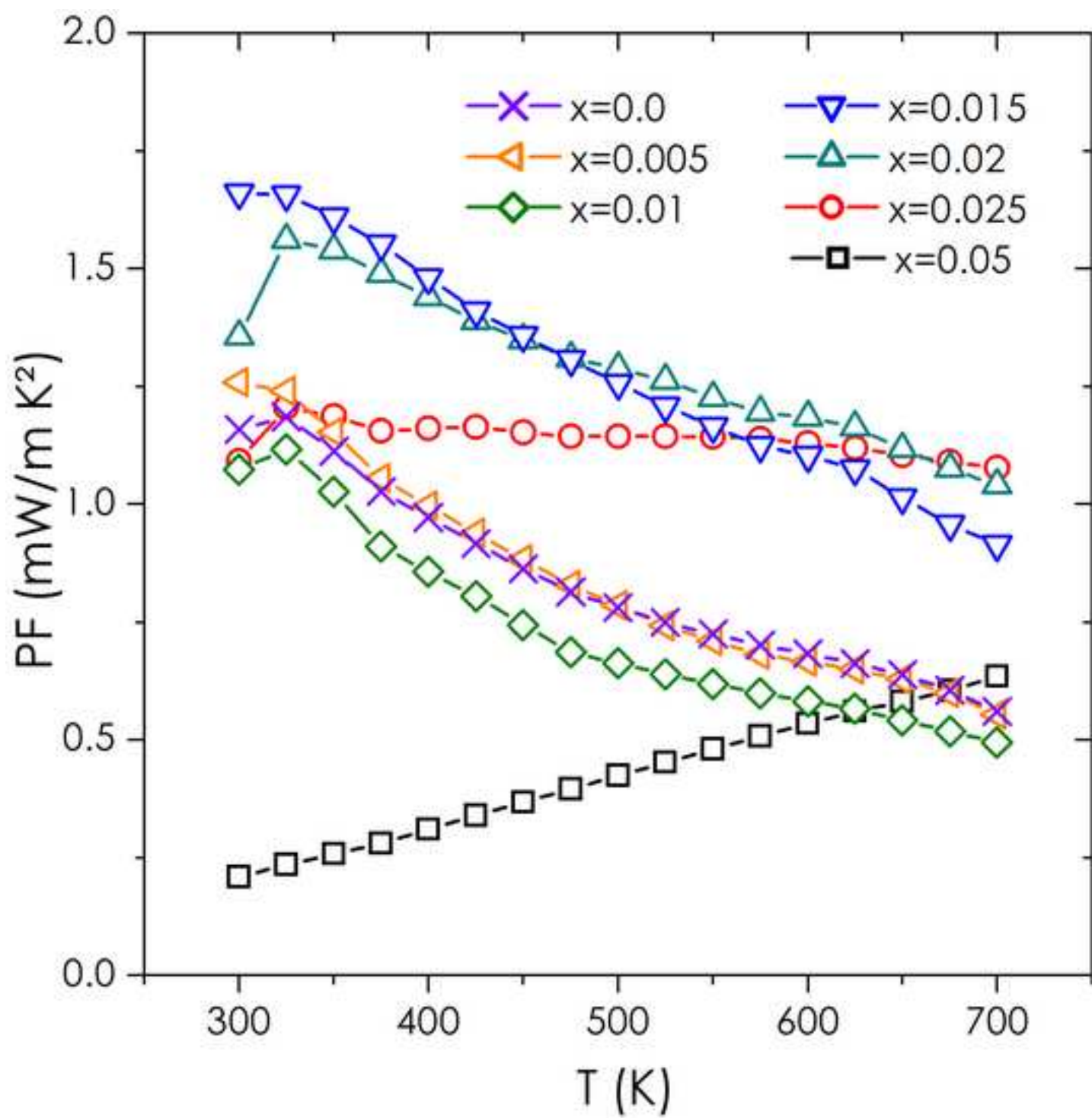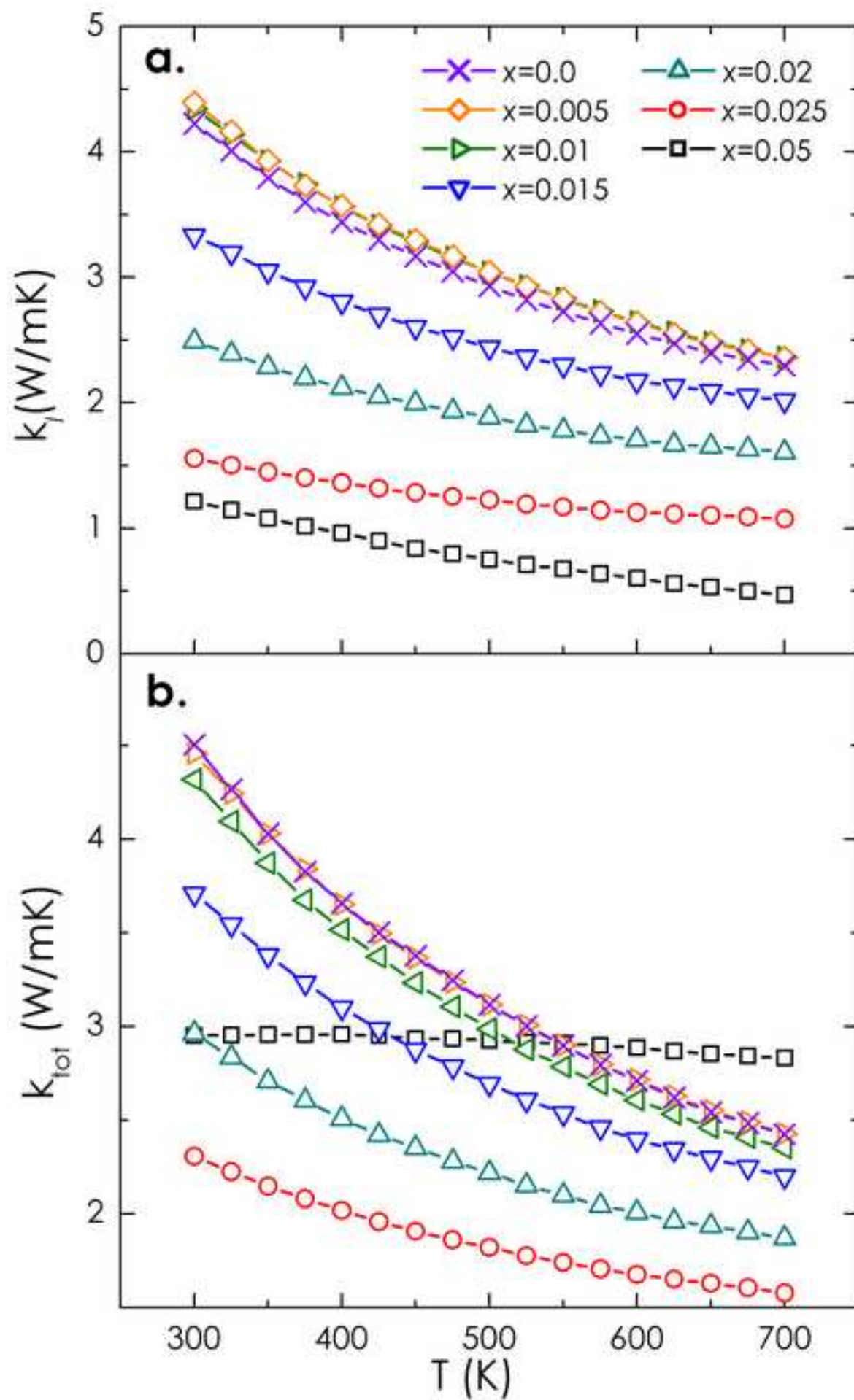**Click here to download high resolution image**
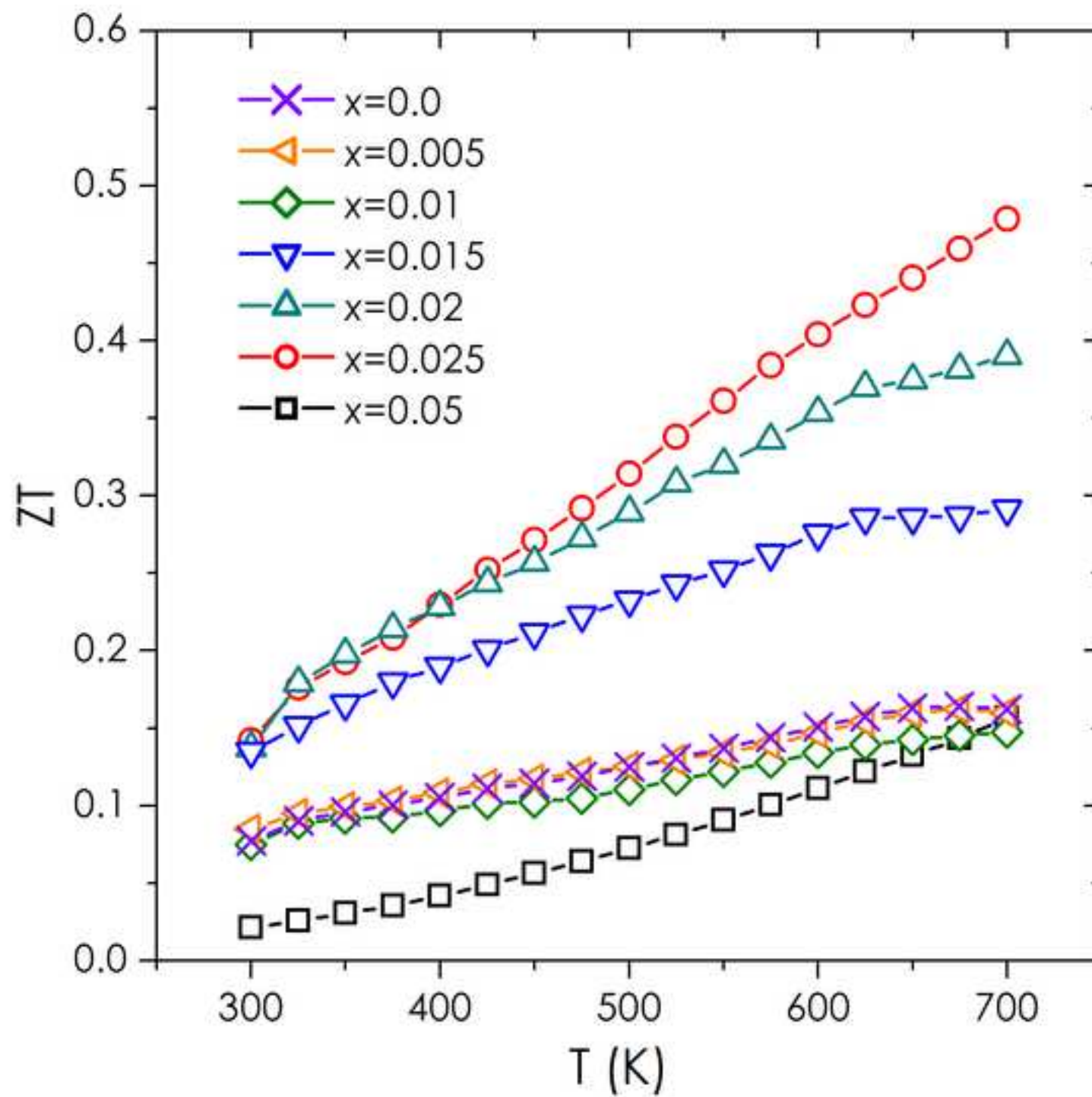
Figure7
Click here to download high resolution image

Figure8
Click here to download high resolution image

Table1

	c parameter Å	ρ mΩcm	S µV/K	κ W/mK	κ_i W/mK	PF mW/mK²	ZT	n (300K) x 10²¹ cm⁻³
x=0	5.678(1)	26.8	-388	2.43	2.36	0.56	0.16	0.11
x=0.005	5.684(1)	26.0	-380	2.43	2.36	0.55	0.16	0.13
x=0.01	5.685(1)	31.1	-392	2.35	2.30	0.50	0.15	0.16
x=0.015	5.700(1)	9.4	-293	2.20	2.02	0.91	0.29	0.46
x=0.02	5.700(1)	6.6	-262	1.87	1.61	1.04	0.39	0.52
x=0.025	5.701(1)	3.42	-192	1.58	1.08	1.08	0.48	1.11
x=0.05	5.715(1)	0.73	-68	2.83	0.47	0.63	0.16	12.2